Int. J. Advanced Design and Manufacturing Technology, 2023, Vol. 16, No. 1, pp. 57-64

DOI: 10.30486/admt.2023.1963260.1368 ISSN: 2252-0406 https://admt.isfahan.iau.ir

Design Construction and Evaluation of a Ring-like Karbandi Structure

Ahad Shah Hosseini[1,] *, Sajjad Pakzad[2]
Faculty of Design, Tabriz Islamic Art University, Iran
E-mail: ahad.shahhoseini@tabriziau.ac.ir, s.pakzad@tabriziau.ac.ir
*Corresponding author

Mohammad Mahdi Ranjbar Malek Shahi[3]
Faculty of Design, Tabriz Islamic Art University, Iran
E-mail: mm.ranjbar@tabriziau.ac.ir

Received: 16 July 2022, Revised: 18 October 2022, Accepted: 23 October 2022

Abstract: Due to the gold price increases in the Iranian market, the desired buyers have been attracted to LGJ (Lightweight Gold Jewelry). Meanwhile, because of the strength decreases in structure in LGJ., we investigated a structural solution in this research. The proposed solution was Karbandi as a supporting lattice-ordered structure in Iranian architecture. We used five types of primary Iranian architecture arches and a perfectly logical Karbandi plan to create ring-like structures. Arches and ring-like structures were compared based on maximum mises stress, strain, and weight using FEM analyses. The applied load and approximate area of it in analyses, according to the female mean Tip-pinch and the mean of minimum, thumb, and index finger width were chosen. Based on analyses results, a ring-like Karbandi structure was chosen for construction. The models were constructed in four alloys category based on sterling silver standard with Cu-nanoparticles as an admixture. A practical test was done to investigate the mean deformation time for each alloy's model category. A weight was used to investigate the observable deformation time-based capacity of the models. Results showed that the lowest mises max stress value was observed in the 1st arch, although the 3rd arch had the minimum strain among arches. In ring-like Karbandi structures made from 1st and 3rd arches, the minimum value of mises max stress and strain was related to the Karbandi. In the physical load applying process, the category that did not contain cu-nanoparticles had the highest deformation meantime among all categories.

Keywords: FEM Analyses, Iranian Architecture, Karbandi, Ring, Structure

Biographical notes: Ahad Shahhoseini received his Ph.D. in Architecture from Sapienza University of Rome, Rome, Italy, in 2012. He is currently an assistant professor in the Faculty of Design at Tabriz Islamic Art University, Tabriz, Iran. His research interests include Industrial Design, Eco-Design, and Design studies. **Sajjad Pakzad** received his Ph.D. in Mechanical Engineering from University of Tabriz, Tabriz, Iran, in 2018. He is currently an assistant professor in the Faculty of Design at Tabriz Islamic Art University, Tabriz, Iran. His research interests include Industrial Design, Parallel Mechanisms, and Robotics. **Mohammad Mehdi Ranjbar Malek Shahi** received his B.Sc. in Industrial Design from Tabriz Islamic Art University in 2020. He is currently an MSc student in industrial Design at the Faculty of Design at Tabriz Islamic Art University, Tabriz, Iran. His research interests include Design studies, mechanical structures, mechanical mechanisms and FEM analyses spatially in gold ornaments and Jewelry.

Research paper

1 INTRODUCTION

The price of gold in the Iranian market has increased significantly in recent years [1]. Hence, the desire of buyers and subsequent, production has been attracted to "lightweight gold jewelry" (LGJ.). Making LGJ. due to the metal and mechanical properties of gold alloy used in the Iranian market [2], structurally has reduced the strength of jewelry. One of the characteristics of buyers of LGJ., in particular a ring, is its relative observable mechanical strength against the normal pressure that is applied to both sides of the ring with two fingers. The result of this process is influential on buying willingness. Using lattice structures, it is possible to have lightweight and high strength together [3]. In many design applications, lattice structures are used for their excellent properties including the light-weighting, high specific strength, stiffness [4] and their positive effects on the total deformation capacity [5]. Therefore, in this study, we investigated the effects of a supporting lattice-ordered structure of Iranian architecture in LGJ. mechanical behavior. The selected structure was Karbandi. Karbandi is one of the supporting structures in Iranian architecture [6]. Each Karbandi structure is composed of arches [7]. Five types of arches were introduced in Jamshid Kashani's book "Mafatih al-Hesab" and considered as Karbandi basis in Iranian architecture [8]. These five arches were simulated in "Rhinoceros 7" software according to details and drawing methods presented in the partial translation of Mafatih al-Hesab [9]. The simulation results were compared using the Finite Element Method (FEM) analyses in Abaqus software. The criteria were maximum mises stress, strain, and weight at the same load, thickness, and material mechanical properties. The load applied to the samples was taken from a study that measured females' tip-pinch in Tabriz [10].

According to the results of the pre-stage (minimum of strain and mises stress), in this paper we selected two arches and used them to design a Karbandi structure with the most similarity to a women's gold ring. Then, due to a certain limit of the criteria and construction limitations of the ring, we chose one model for construction. Alloys in jewelry industry usually are made by using bulk metals as an admixture [11]. The overall positive strengthening effect of metal nanoparticles on alloys has been investigated [12]. Thus, for investigating the effects of nanoparticles on the deformation capacity of metals used in the jewelry industry we used silver (as base metal) Cu, and Cu-nanoparticles (as admixture) to make models in four different alloy types. Finally, we compared these four models' deformation capacity by a practical load applying procedure.

2 AN IRANIAN ARCHITECTURE SUPPORTING STRUCTURE

2.1. Arches

Arches are one of the first steps of development in architectural structures [13]. Ghiyath al-Din Jamshid Kashani (1380-1429) wrote a manuscript known as "Miftah al-hisab" (Key of Arithmetic) and introduced five main types of arches in Islamic architecture and methods of drawing them [8]. We use these arches types and methods of drawing in this study ("Fig. 1").

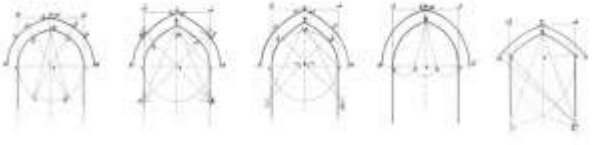

Fig. 1 Types of arches in the Persian translation of "Miftah al-hisab" [9].

2.2. Karbandi Structure

Karbandi is one of the identity elements of Iranian architecture that integrates architecture and structure and it is based on two criteria, a plan of n-sided Karbandi and an arch [7]. Plan of each n-sided Karbandi based on a circle that is divided into "n" equal parts. From a selected point of division, a connection distance is equal to "d" (which connects one point to another desired point), arches are placed on this distance, and circular arrayed "n" times. The shape with the sides of "a" and "b" are used to delete unwanted pieces according to the type of Karbandi ("Fig. 2").

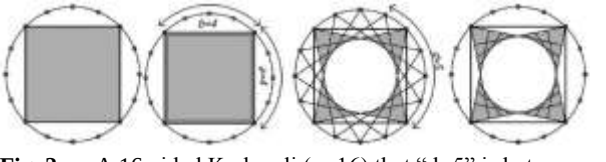

Fig. 2 A 16-sided Karbandi (n=16) that "d=5" is between "a=4" and "n/2=8" [7].

If "d" is between "a" and "n/2" then, the Karbandi is perfectly logical and geometrically correct [7]. We use this type of Karbandi to create a ring-like structure.

3 2D AND 3D MODELING

3.1. Arches Modelling

Two-dimensional Modeling of arches was done in generic overall dimensions in "Rhinoceros 7" according to "Miftah al-hisab" instructions ("Fig. 3").

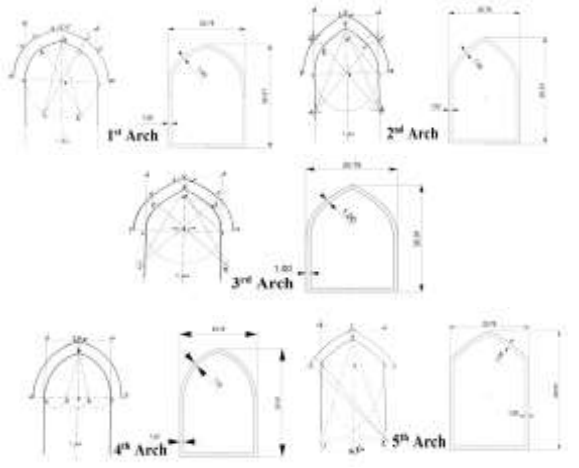

Fig. 3 Arches (left column) [9] and 2D modeling of them (right column) with "Rhinoceros 7".

3.2. Ring-Like Karbandi Structures

Using the geometrical perfect type of Karbandi [7], arches mentioned in the previous section, and "Rhinoceros 7" as 3D modeling software, the ring-like Karbandi structures were modeled. The plan of Krabandi is a 16-sided (n=16) and parameters "a" and "b" are set to 4 (a=b=4). The Karbandi circle diameter is 26.56 mm according to the ring size 59 (by European standard). All possible "d" quantities (d = 2, 3, 4, 5, 6, and 7) are considered due to the "a<d<n/2" relation. Finally, the deletion method and bottom connection of each structure were considered based on a ring-like shape creation ("Fig. 4" and "Fig. 5").

Fig. 4 Ring-like Karbandi structure created with specifications of a=b=4, d=6 and using the first arch in "Fig. 3".

Fig. 5 Ring-like Karbandi structures base on the first arch with all "d" possible quantities (d=2, 3, 4, 5, 6 and 7, left to right accordingly).

4 FINITE ELEMENT ANALYSES

4.1. Software and Analyses Specifications

We used "Abaqus DS Simulia Suite 2022" for all analyses in this study. All 2D and 3D models were converted to IGES. format for importing to Abaqus. The category of section applied to all models and their types were Shell and Homogenous, respectively. The Shell thickness is set to 0.3 mm based on a common gold ring shell thickness. All analyses were static in the category of mechanical. The meshing technique is set to free and "Tri" type, and mesh types were standard linear shells. The requested output fields were "Maximum Mises equivalent stress", "E, Max" (strain), and also weight calculated in the software environment.

4.1.1. Applied Load (Amount, Location, and, Direction)

Duo to the Tip-pinch which has the most similarities to fingers position in ring-wearing posture, we used the results of a cross-sectional study that took place in Tabriz which was conducted among 196 (96 males and 100 females) volunteers. The applied load and approximate area of it, according to the female mean Tip-pinch (4.7 Kgf[1] = 46.09 N) and the mean of minimum, thumb, and index finger width were chosen [10]. The mean amount of thumb and index finger width (1.3 cm) was used as the applying load area. ("Fig. 6").

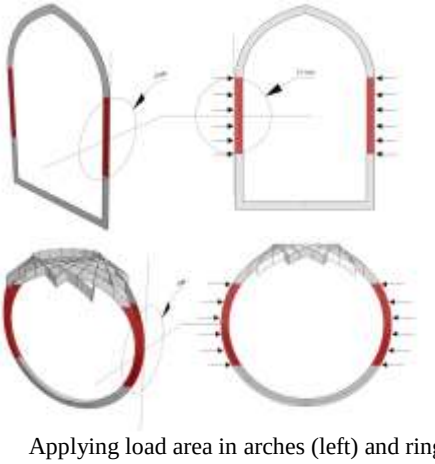

Fig. 6 Applying load area in arches (left) and ring-like Karbandi structure (right).

Exhaustive researches have been done on the behavior of arches under vertical loads [14-17] but less attention has been devoted to their horizontal endurance [18]. In this study due to fingers condition in ring-wearing posture (thumb and index finger), we considered the load direction horizontally symmetrical to structures at the applying load areas ("Fig. 6").

4.1.2. Material Properties

The most common precious metals in the fine jewelry industry are gold, platinum, palladium, and silver [19]. We used gold mechanical properties data ("Table 1") from the CATIA material library in all FEM analyses [20].

Table 1 Gold mechanical properties

Material	Gold
Density (kg/m^3)	19320
Young's modulus (N/m^2)	7.8e+10
Poisson's ratio	0.42
Yield stress (N/m^2)	2.05e+8

5 CONSTRUCTION PROCESS

5.1. Alloy Specifications and Categories

A decrease in structure weight can be the cause of a decrease in its strength [21], one solution to overcome this, is using alloys with more stiffness (less deformation capacity). Due to reduced production costs in this study, we used sterling silver alloy to construct ring-like structures. Sterling silver is an alloy of silver and copper, known as silver 925 which contains 92.5% silver and 7.5% copper by weight [22]. Copper is a metal that exists in both gold and silver alloys as an admixture [22], hence, its degree of mixture variation can be generalizable for gold alloys' capacity of deformation too.

The positive effects of metal nanoparticles on the mechanical behavior of alloys have been investigated [12-24]. Thus, in this study, we used some variations of copper and its nanoparticles to investigate their effect on the deformation capacity of ring-like Karbandi structures.

The melting point of metal nanoparticles is lower than the bulk metal and has a direct relationship with their size of it [25]. Thus, with increases in metal nanoparticle size, the melting point temperature is increased. Due to the preservation of metal nanoparticle properties because of the close melting point temperature of silver and copper (Ag, 961.78 °C and Cu, 1.085 °C), we used the largest Cu-nanoparticles size (100 nm) available on the market ("US NANO" brand) and to ensure purity, Cu-microparticles ("Armina" brand) in constructing categories of sterling silver alloys ("Table 2").

Table 2 Categories of sterling silver alloys (based on 20 g weight of each category).

Categories	Silver	Cu-Nanoparticles	Cu-Microparticles
First	18.5 G	-	1.5 G
Second	18.5 G	1.5 G	-
Third	18.5 G	1 G	0.5 G
Fourth	18.5 G	0.5 G	1 G

5.2. 3D Printing

We used the "Form Labs 2" 3D printer for printing the models. The resin brand was similar to the 3D printer (purple castable wax). Totally 24 models were printed (6 models for each alloy category). The thickness of the layers was 50 µm, the total number of them was 530 and, 32 mL resin was used for the 3D printing process.

5.3. Casting Process Specifications

We used a vacuum casting machine and oxy-acetylene torch for melting silver and copper (nanoparticles and microparticles) in the casting process. The casting plaster brand was Optima (green model-resin specific) and 1 kg plaster was used for each casting process (a total of 4 casting process was done). A 10 centimetres height flask was used for casting. Baking time and casting temperatures were 7 h and 720 °C, respectively, and casting was done under 600 psi vacuum pressure ("Fig. 7").

Fig. 7 Several views of a casting model (first alloy's category).

6 PRACTICAL LOAD APPLICATION

To investigate the observable deformation of constructed models (in 4 alloys categories), we used a dial thickness gauge (0-20 mm range - 0.1 mm graduation), standard 50 g, and 2000 g (about 40% of Tip-pinch [10]) calibration weights and a mini table clamp. The 50 g calibration weight was used to measure the models' diameter in the initial state, then the 2000 g weight was used to investigate the observable deformation capacity of the models. All models of each alloy's category were used to calculate the mean (time-based) deformation capacity ("Fig. 8").

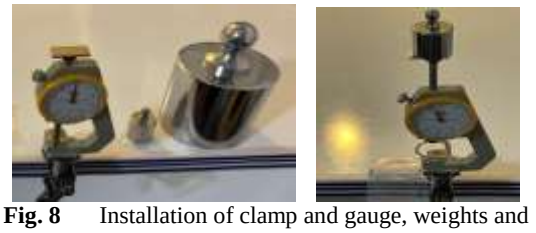

Fig. 8 Installation of clamp and gauge, weights and models (we used a neodymium magnet (1.3g) for more fixity of weights during measurement).

7 RESULTS

7.1. Software Analyses

7.1.1. Arches

The results of finite element method analyses for maximum Mises stress, maximum strain, and weight

calculation of each arch were shown ("Fig. 9" and "Table 3").

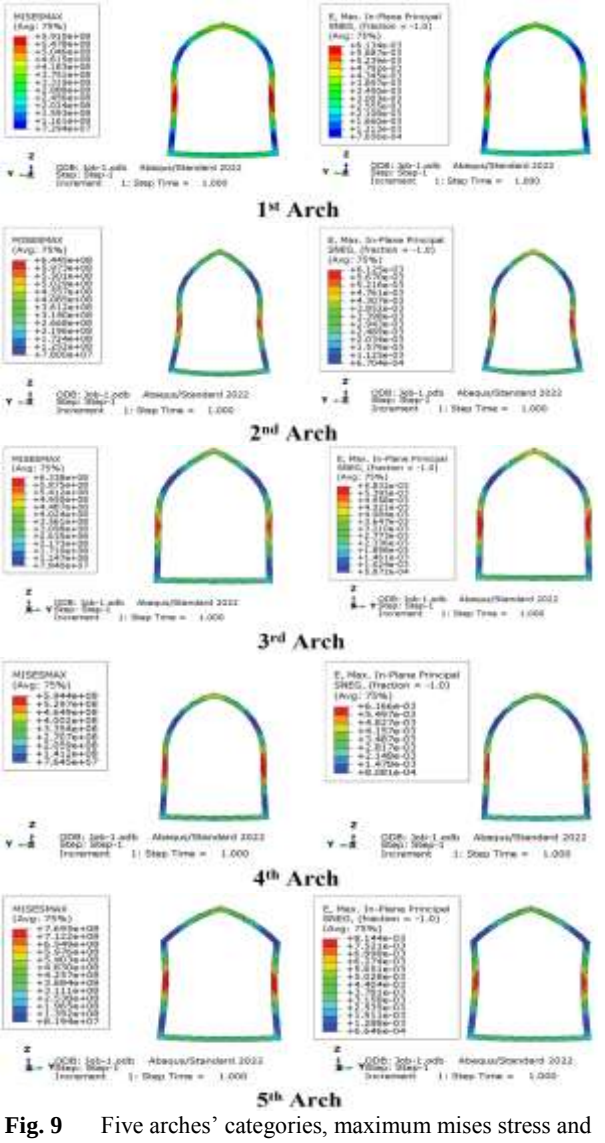

Fig. 9 Five arches' categories, maximum mises stress and maximum strain.

Table 3 Arches' mises max, strain, and weight

Arches	Mises Max (N/m^2)	Strain	Mass (Kg)
1	5.910e+8	6.134e-3	5.54e-4
2	6.445e+8	6.125e-3	5.43e-4
3	6.338e+8	5.832e-3	5.42e-4
4	5.944e+8	6.166e-3	5.49e-4
5	7.695e+8	8.144e-3	5.57e-4

Two aches with the minimum of mises max stress (1st arch) and a minimum of strain (3rd arch) were used to create ring-like Karbandi structure variations.

7.1.2. Ring Like Karbandi Structures

The results of finite element method analyses for maximum von mises stress, maximum strain, and weight calculation of each ring-like Karbandi structure with all "d" possible quantities (d=2, 3, 4, 5, 6, and 7) were shown ("Fig. 10", "Fig. 11", "Fig. 12", "Fig. 13" and "Table 4").

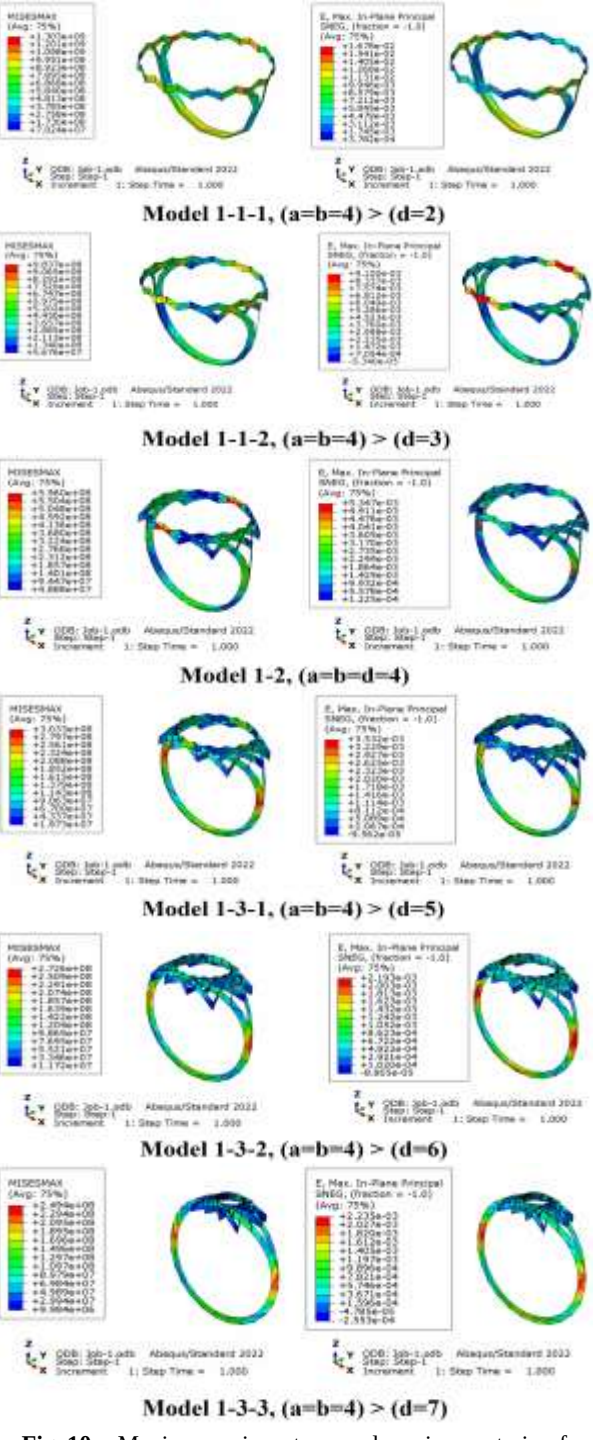

Fig. 10 Maximum mises stress and maximum strain of ring-like Karbandi structures with all "d" possible quantities (d=2, 3, 4, 5, 6 and 7) using the 1st arch.

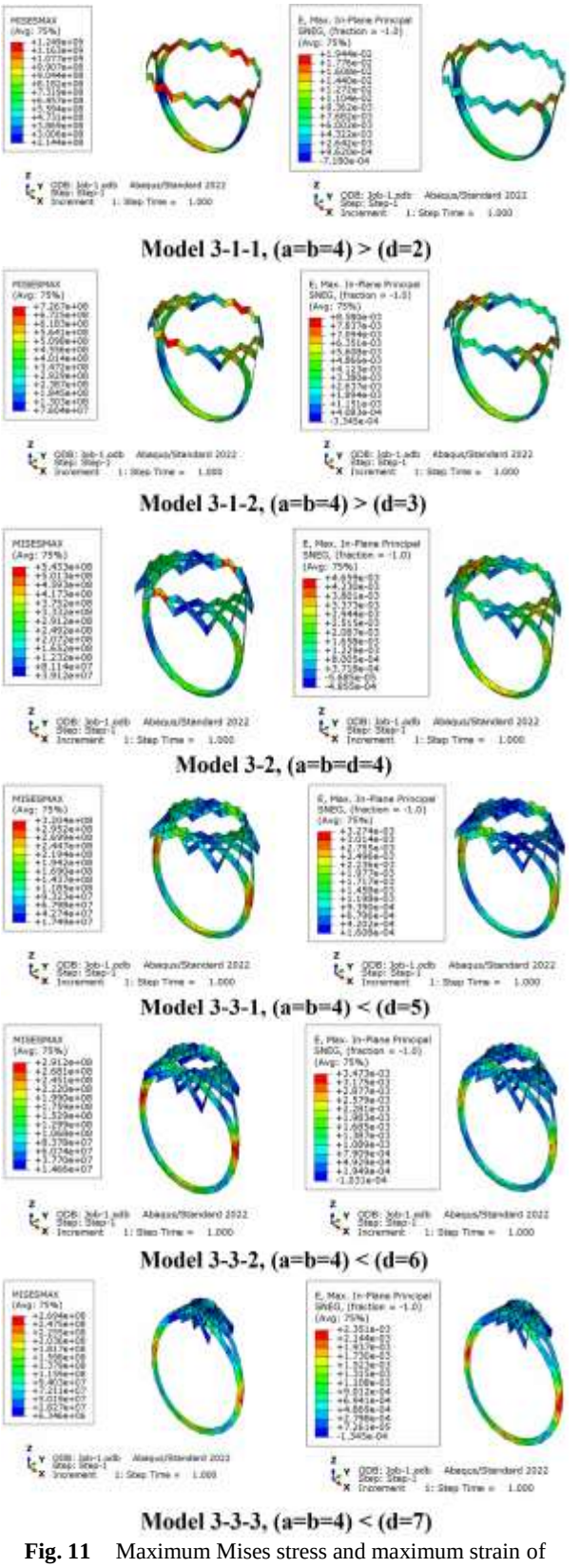

Fig. 11 Maximum Mises stress and maximum strain of ring-like Karbandi structures with all "d" possible quantities (d=2, 3, 4, 5, 6 and 7) using the 3rd arch.

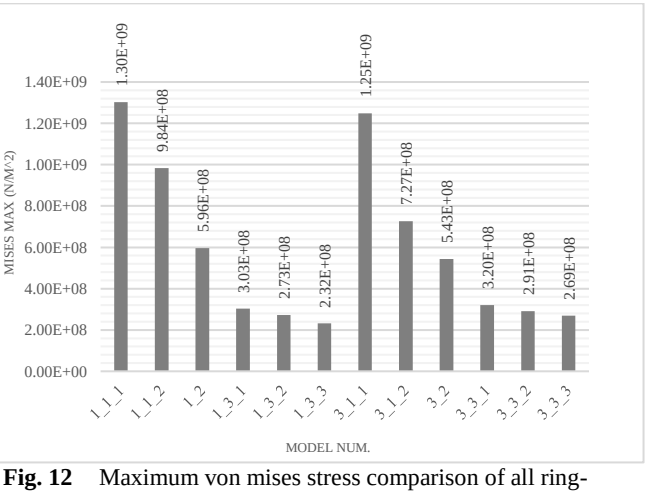

Fig. 12 Maximum von mises stress comparison of all ring-like Karbandi structures.

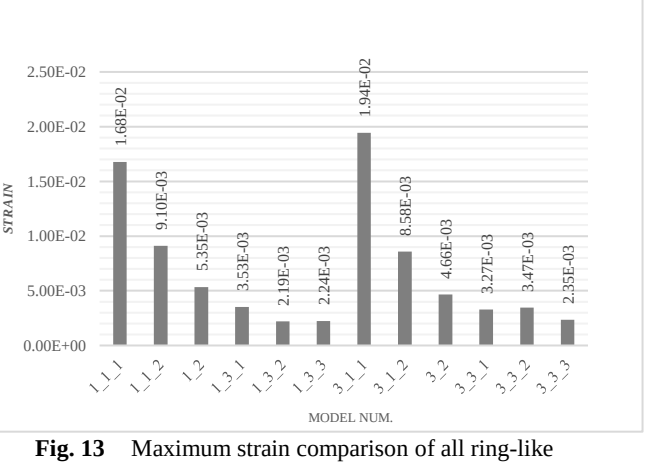

Fig. 13 Maximum strain comparison of all ring-like Karbandi structures**.**

Table 4 Ring-like Karbandi structures von mises maximum stress, strain, and weight

Model Num.	Mises Max (N/m^2)	Strain	Weight (kg)
1_1_1	1.30E+09	1.68E-02	9.24E-04
1_1_2	9.84E+08	9.10E-03	1.13E-03
1_2	5.96E+08	5.35E-03	1.42E-03
1_3_1	3.03E+08	3.53E-03	1.65E-03
1_3_2	2.73E+08	2.19E-03	1.71E-03
1_3_3	2.32E+08	2.24E-03	1.52E-03
3_1_1	1.25E+09	1.94E-02	9.93E-04
3_1_2	7.27E+08	8.58E-03	1.20E-03
3_2	5.43E+08	4.66E-03	1.52E-03
3_3_1	3.20E+08	3.27E-03	1.76E-03
3_3_2	2.91E+08	3.47E-03	1.82E-03
3_3_3	2.69E+08	2.35E-03	1.62E-03

7.2. Practical Experiments

The results of all model's diameters on 50 g and their mean deformation time on 2000 g weights are shown ("Fig. 14" and "Table. 5").

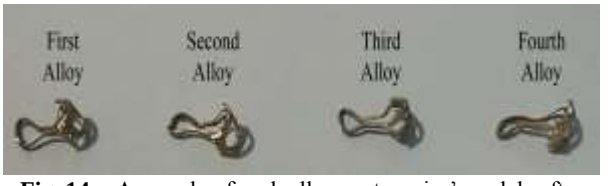

Fig. 14 A sample of each alloys categories' models after deformation.

Table 5 Admixtures weight (base metal, MP (microparticles), and NP (nanoparticles)), the diameter of models on 50 g and 2000 g weights, and deformation mean time of each 6 models of each category

Alloys category	Admixtures' weights	D on 50 g	D on 2000 g	Meantime (S)
First	18.8g Ag + 1.5g Cu(MP)	19.3mm	Pressed	3.97
Second	18.8g Ag + 1.5g Cu(NP)	19.4mm	Pressed	1.96
Third	18.8g Ag + 1g Cu(NP) + 0.5g Cu(MP)	19.3mm	Pressed	2.23
Fourth	18.8g Ag + 1g Cu(MP) + 0.5g Cu(NP)	19.5mm	Pressed	2.77

8 CONCLUSIONS

Using structures as a combination of members connected in such a way to support more loads can be a solution to increase solidity in LGJ. In this research, we tried to introduce a structure for this problem. The proposed structure was Karbandi. Arches and Karbandi-plan as the most important factors in this structure were investigated. The results showed that in the first arch, the lowest mises max stress value was observed due to the application of the same load, and the arch's weight was fourth among the five weights. Although the third arch had the minimum strain and the lowest weight among arches. In model 1-3-3 from ring-like Karbandi structures, the lowest mises max stress value was observed and it had the fifth place in terms of the most weight. In model 1-3-2, the lowest strain value was observed and it had the sixth place in terms of the most weight in its category (ring-like Karbandi structures based on the first arch). The minimum value of mises max stress and also strain was related to the Karbandi plan with the "(a=b) < d" relation. This condition was observable in structures that were made from the first and third arches.

In the physical load applying process, because of clamp surface decrease of load applying area to approximately 1/12 of the area considered in the FEM analyses, the physical stress increased 12 times and an inevitable complete deformation occurred. The first category that did not contain cu-nanoparticles had the highest deformation meantime among all categories. The lowest deformation meantime was related to the second category that contains the most Cu-nanoparticles as an alloy's admixture. Also, in the third and fourth alloy categories, it is observable that the more presence of Cu-nanoparticles led to increase in deformation meantime. One cause of this phenomenon can be the airflow in the oxy-acetylene flame. Because of the very low weight of nanoparticles, this flow can pour out Cu-nanoparticles out of the melting pot before the melting process. On the other hand, the flammability of Cu- nanoparticles can be the reason for the lack of influence or the absence of Cu-nanoparticles' mechanical properties in the alloy categories.

APPENDIX

[1]. Kgf (Kilogram-Force) is a non-SI dimension of force that is generally used in medical research and is equal to the magnitude of the force exerted on one kilogram of mass in a 9.80665 m/s^2 gravitational field [26].

ACKNOWLEDGMENTS

We acknowledge the Islamic Art University of Tabriz, the Design department, and Skyseas gold gallery, for supporting this work.

REFERENCES

[1] Dastranj, E., Sahebi Fard, H., Abdolbaghi, A., and Reza Hejazi, S., Power Option Pricing Under the Unstable Conditions (Evidence of Power Option Pricing Under Fractional Heston Model in The Iran Gold Market), Physica A: Statistical Mechanics and its Applications, Vol. 537, 2020, pp. 122690, https://doi.org/10.1016/j.physa.2019.122690.

[2] Saradesh, K., Vinodkumar, G., Metallurgical Processes for Hardening of 22karat Gold for Light Weight and High Strength Jewelry Manufacturing, Journal of Materials Research and Technology, Vol. 9, No. 2, 2020, pp. 2009-2020, https://doi.org/10.1016/j.jmrt.2019.12.033.

[3] Pan C, Han Y, Lu J., Design and Optimization of Lattice Structures: A Review, Applied Sciences, Vol. 10, No. 18, 2020, pp. 63-74, https://doi.org/10.3390/app10186374.

[4] Dong, G., Yunlong, T., and Yaoyao F. Zh., A Survey of Modeling of Lattice Structures Fabricated by Additive Manufacturing, Journal of Mechanical Design, Vol. 139, No. 10, 2017, 100906.

[5] Großmann, A., Gosmann, J., and Mittelstedt, C., Lightweight Lattice Structures in Selective Laser Melting: Design, Fabrication and Mechanical

Properties, Materials Science and Engineering: A, Vol. 766, 2019, pp. 138356, https://doi.org/10.1016/j.msea.2019.138356.

[6] Pour Ahmadi, M., Sohrabi, M., Design of Persian Karbandi: The Problem of Dividing the Base from a Mathematical Viewpoint, Jria.iust.ac.ir. Vol. 7, 2019, pp. 21-36, Online access, http://jria.iust.ac.ir/article-1-1171-en.html.

[7] Amjad Mohamadi, A., Nejad Ebrahimi, A., and Shahbazi, Y., Geometric Design of a Masonry Lattice Space Dome Titled Karbandi in Persian Architecture, International Journal of Space Structures, Vol. 34, No. 2, 2019, pp. 22-39, https://doi.org/10.1177/0956059919845631.

[8] Koliji, H. Revisiting the Squinch: From Squaring the Circle to Circling the Square, Nexus Netw Journal, Vol. 14, 2012, pp. 291–305, https://doi.org/10.1007/s00004-012-0113-9.

[9] Jazbi, A., Risaaleh Taaq va Ajaz, Soroush Publications, Tehran, Iran, 1987, pp. 27 (Partial Translation of Miftah al-hisab).

[10] Maleki-Gahfarokhi, A., Dianat, I., Feizi, H., and Asghari-Jafarabadi, M., Influences of Gender, Hand Dominance, and Anthropometric Characteristics on Different Types of Pinch Strength: A Partial Least Squares (PLS) Approach, Applied Ergonomics, Vol. 79, 2019, pp. 9-16, https://doi.org/10.1016/j.apergo.2019.04.002.

[11] Klotz, U. E., Tiberto, D., and Held, F., Optimization of 18-Karat Yellow Gold Alloys for The Additive Manufacturing of Jewelry and Watch Parts, Gold Bull, No. 50, 2017, pp. 111–121 https://doi.org/10.1007/s13404-017-0201-4.

[12] Pang, X., Xian, Y., Wang, W., and Zhang, P., Tensile Properties and Strengthening Effects of 6061Al/12 wt%B4C Composites Reinforced with Nano-Al2O3 Particles, Journal of Alloys and Compounds, Vol. 768, 2018, pp. 476-484, https://doi.org/10.1016/j.jallcom.2018.07.072.

[13] Buzurgmehri, Z., Hindisa dar Mimari (Geometry in Persian Architecture), Iranian Cultural Heritage Organization, Tehran, Iran, 1992, pp. 154 (In Farsi).

[14] Marano, G. C., Trentadue, F., and Petrone, F., Optimal Arch Shape Solution Under Static Vertical Loads, Acta Mech, Vol. 225, 2014, pp. 679–686, https://doi.org/10.1007/s00707-013-0985-0.

[15] Guo, Y., Chen, H., Pi, Y., and Bradford, M., In-Plane Strength of Steel Arches with a Sinusoidal Corrugated Web Under a Full-Span Uniform Vertical Load: Experimental and Numerical Investigations, Eng Struct, Vol. 110, 2016, pp.105-115, https://doi.org/10.1016/j.engstruct.2015.11.056.

[16] Marano, G., Trentadue, F., Greco, R., Vanzi, I., and Briseghella, B., Volume/Thrust Optimal Shape Criteria for Arches Under Static Vertical Loads, Journal of Traffic and Transportation Engineering (English Edition), Vol. 5, 2018, pp. 503-509, https://doi.org/10.1016/j.jtte.2018.10.005.

[17] Zampieri, P., Tetougueni, C., Maiorana, E., and Pellegrino, C., Post-Buckling of Network Arch Bridges Subjected to Vertical Loads, Structure and Infrastructure Engineering, Vol. 17, 2020, pp. 941-959, https://doi.org/10.1080/15732479.2020.1778742.

[18] Brandonisio, G., Mele, E., and De Luca, A., Limit Analysis of Masonry Circular Buttressed Arches Under Horizontal Loads, Meccanica, Vol. 52, 2017, pp. 2547-2565, https://doi.org/10.1007/s11012-016-0609-6.

[19] Sensoy, A., Dynamic Relationship Between Precious Metals, Resources Policy, Vol. 38, 2013, pp. 504-511, https://doi.org/10.1016/j.resourpol.2013.08.004.

[20] CATIA, Material Library (Mechanical properties), Dassault Systemes, Package 3, Ver. 5-6, Service Pack 1, 2021.

[21] Addisu, H., Koricho, E., Structural Weight and Stiffness Optimization of a Midibus Using the Reinforcement and Response Surface Optimization (RSO) Method in Static Condition, Modelling and Simulation in Engineering, Vol. 2022, 2022, pp. 1-15, https://doi.org/10.1155/2022/6812744.

[22] Grimwade, M., Introduction to Precious Metals; Metallurgy for Jewelers and Silversmiths, Brynmorgen press, USA, First Edition, 2009, pp. 91-102.

[23] Aarts, W., Jarvis, R., The Change in Resistivity, On Plastic Deformation, Of Silver-Copper and Silver-Gold Alloys, Acta Metallurgica, Vol. 2, No. 1, 1954, pp. 87-91, https://doi.org/10.1016/0001-6160(54)90098-x.

[24] Gain, A., Zhang, L., The Effects of TiO2 Nanoparticles Addition on The Thermal Shock Resistance, Shear Strength and IMC Layer Growth of SAC305 Alloy, Materialia (Oxf), Vol. 3, 2018, pp. 64-73, https://doi.org/10.1016/j.mtla.2018.10.009

[25] Aliofkhazraei, M., Handbook of Nanoparticles, Springer Cham, 2020, pp. 664-665, https://doi.org/10.1007/978-3-319-13188-7.

[26] Cholewickl, J., Wolf, S., Unit of Measurement: Newton (N) Versus Kilogram Force (kgf), Journal of Hand Surgery, Vol. 23, No. 5, 1998, pp. 952, https://doi.org/10.1016/s0363-5023(98)80181-0.